Available online at www.sciencedirect.com
ScienceDirect
Journal of Power Sources 175 (2008) 773–778
JOURNAL OF POWER SOURCES
www.elsevier.com/locate/jpowsour

Short communication

Surrogate model for proton exchange membrane fuel cell (PEMFC)

R. Tirnovan, S. Giurgea*, A. Miraoui, M. Cirrincione

Institut FC LAB, UTBM Laboratory, University of Technology of Belfort-Montbéliard (UTBM), Thierry Mieg 90010, Belfort Cedex, France

Received 22 June 2007; received in revised form 20 September 2007; accepted 23 September 2007
Available online 5 October 2007

Abstract

The main goal of this work is to realize a PEMFC model that can be used efficiently for the global modelling of the fuel cell system. The modelling method proposed in the paper is an approach from an empirical point of view that allows a PEMFC model of "black-box" class to be developed. Moving least squares (MLS) have therefore been employed to approximate the cell voltage characteristics *V*, using an experimental dataset measured in determinate conditions. The MLS approach appears to present a good balance of response surface accuracy, smoothness, robustness, and ease of use. This kind of numerical model offers good perspectives for the systems identification, the simulation of the systems, the design and the optimization of process control, etc. The results prove that the method is suitable for predicting and describing the fuel cell behaviour in all the points of the approximation domain. The proposed model can be included in a numerical application to optimize the operation of an existing fuel cell system.

Keywords: Fuel cell; Moving least squares; Surrogate model; Performance; Prediction

1. Introduction

Fuel cells power generating systems represent a solution to replace traditional distributed power sources because of their high efficiency, clean operation and multiple applications (transport, residential, portable) [1,2]. Fuel cell based power plants are currently under rapid development and first plants are expected by the next few years with size ranging from 20 to 250 kW, up to 1 MW [2]. In particular, proton exchange membrane fuel cells (PEMFC) are most suitable for automotive applications because of their low operation temperature, providing a fast start-up, and high power density. The design and analysis of a complete fuel cell system demand the correct modelling of the fuel cell stack and of the other sub-systems around.

Over the last 17 years, many PEMFC models, either theoretical or empirical, from simple zero-dimensional to complex three-dimensional models, have been developed (analytical models, mechanistic models, semi-empirical and empirical models). There are several papers which review some of the work about PEMFC modelling, for example [3,4]. Semi-empirical approaches combine theoretically derived differential and algebraic equations with empirically determined relationships [5–9]. The empirical approaches develop algebraic models based on experimental datasets. They describe the performance of a true system working in given conditions. Such models can be based on analytical expressions [10] or they can be described by pure numerical approaches.

The main goal of this work is to realize a PEMFC model that can be used efficiently for the global modelling of the fuel cell system. The modelling method proposed in the paper is an approach from an empirical point of view that allows PEMFC model of "black-box" class to be developed. The MLS approximation method is the core of the proposed method. The MLS method is widely used in meshless methods but it has been successfully applied for response surface generation in the context of optimization [11]. The MLS algorithm uses an experimental dataset, cell voltage versus current density, measured in determinate experimental conditions (pure hydrogen fuel, air as oxidant, cell temperature, pressure, membrane humidity, reactants stoichiometry), in order to create the PEMFC numeric model. Such numerical models are extensively employed in various areas of the science and of the technology offering good perspectives in the systems identification, the simulation of the systems, the design and the optimization of process control, etc. The proposed model can be included in a numerical application to optimize the operation of an existing fuel cell system.

* Corresponding author. Tel.: +33 384 58 36 40; fax: +33 384 58 34 13.
E-mail address: stefan.giurgea@utbm.fr (S. Giurgea).

0378-7753/$ – see front matter © 2007 Elsevier B.V. All rights reserved.
doi:10.1016/j.jpowsour.2007.09.097

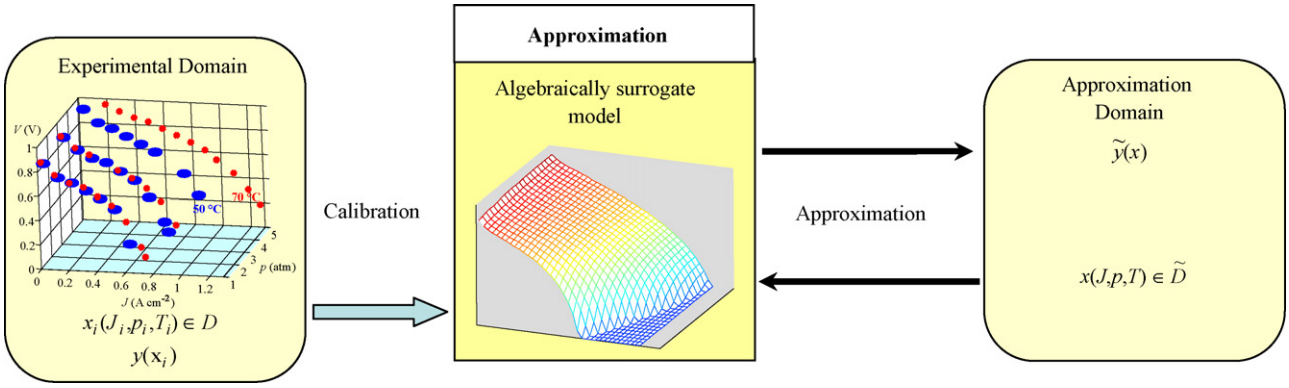

Fig. 1. Application architecture.

2. Analysis and modelling

Based on the MLS method a numerical approximation method for PEMFC modelling has been developed as is shown in Fig. 1.

The central element of this application is the "Approximation" module. This module creates an entity defining algebraically the surrogate model based on the MLS approximation. There are two main operations defined on this surrogate model entity: calibration and approximation. A pre-sampled dataset is needed to calibrate the model. Once calibrated, the algebraic surrogate model provides the "approximation" function that outputs the approximate value and the gradient for every point of the feasibility domain.

2.1. The proposed fuel cell modelling approach

The proposed model belongs to the family of the surrogate models. Most engineering design problems require experiments and simulations to evaluate design objective and constraint functions as function of design variables. One way of alleviating this burden is by constructing approximation models (known as surrogate models, response surface models, metamodels or emulators) that mimic the behaviour of the simulation model as closely as possible. Surrogate models are constructed using a data-driven, bottom–up approach. This approach is also known "behavioural modelling" or "black-box modelling". The most popular surrogate models are polynomial response surfaces, kriging, support vector machines and artificial neural networks [12].

Most of the response surface construction methods use global least squares (GLS) methods. The GLS methods use a single quadratic or cubic polynomial representing the entire parametric space of the random variables. However, the MLS, kriging and radial basis functions (RBF) methods produce higher accuracy in response prediction compared to the GLS methods.

Numerically the MLS and kriging produces the least error. Between kriging and MLS it is difficult to choose one over the other, but MLS consistently produces marginally smaller errors than kriging [13]. Moreover, the MLS metamodelling seems to be more flexible and easy to use than kriging method.

The MLS metamodelling appears to present a good balance of response surface accuracy, smoothness, robustness and ease of use. Therefore, we have used MLS in this paper to generate the response surfaces from our 3D data sets.

This paper proposes and develops a numerical method for modelling the fuel cell. The performance of the fuel cells depends on several factors. The most important factors are the fuel cell operating temperature, the pressure of the reactants, the stoichiometry of the reactants, the nature of the membrane, the humiditification of the membrane, diffusion layer, electrocatalyst layer and the sort of the channels. The proposed method starts from the experimental dataset presented in [6]. This dataset is given in stationary conditions for a PEMFC supplied with hydrogen and air, and it gives measured cell voltage $V = V(J, p, T)$ as a function of the current density J, the air pressure p and the absolute fuel cell temperature T.

As described [6] the experimental dataset were acquired on a PEMFC in the experimental conditions presented in Table 1.

2.2. The moving least squares approximation (MLS) based model

Among the large number of numerical methods about function approximation the moving least squares method provides both an accurate local function approximation and a continuous gradient approximation [11,14–17]. However, also other approximation techniques could be employed like those based on feed-forward neural networks [18,19].

A short overview of the MLS method is exposed below. Considering the sampled dataset $\{(y_i, \mathbf{x}_i)\}_{i=1,\ldots,N}$, where:

- $\mathbf{y} = \{y_i\}_{i=1,\ldots,N} = \{y(\mathbf{x}_i)\}_{i=1,\ldots,N}$ is the vector of function values in the experimental points;
- $\mathbf{x}_i \in D$ is the vector of the coordinates of the i experimental points, with D the experimental domain containing N samples.

According to MLS, the local character is ensured by a weight function $w(\mathbf{x}, \mathbf{x}_i)$ defined on a support region $B(\mathbf{x}_i)$ around $\mathbf{x}_i$:

$$w(\mathbf{x}, \mathbf{x}_i) = w(\mathbf{x} - \mathbf{x}_i) \begin{cases} \geq 0, & \forall x \in B(\mathbf{x}_i) \\ = 0, & \text{if not} \end{cases} \quad (1)$$

Table 1
Experimental conditions [6]

1.	**ELECTRODES**	**Type**	**Area**	**Preparation**
		CESHR, low platinum loading 0.4 Pt mg cm^{-2}	50 cm^2	By the rolling method and impregnated with DuPont Nafion solution
2.	**MEMBRANE**	**Type**	**Relative humidity**	
		Nafion 115	100%	
3.	**CARBON CLOTH SUBSTRATE**	**Teflon content**		
		40 %		
4.	**DIFFUSION LAYER**	**Teflon content**		
		35%		
5.	**ELECTROCATALYST**	**Teflon content**		
		30%		
6.	**FUEL**	**Type**	**Stoichiometric ratio**	
		Hydrogen 99.99% purity	1.2	
7.	**OXYDANT**	**Type**	**Stoichiometric ratio**	
		Oxygen 99.99% purity, or House air	2.0	
8.	**OPERATING TEMPERATURES**	50 °C and 70 °C		
9.	**OPERATING PRESSURES**	1 atm, 3 atm and 5 atm		

with $\mathbf{x}$ the vector of the coordinates of a generic point. This weight function defines a finite domain of influence $B(\mathbf{x}_i) \subset \tilde{D}$, around any experimental point $\mathbf{x}_i$, where $\tilde{D}$ is the approximation domain.

For every point $\mathbf{x}$ of the domain $\tilde{D}$ let $\tilde{y}(\mathbf{x})$ be the moving least squares approximation given by:

$$\tilde{y}(\mathbf{x}) = \sum_{j=1}^{m} p_j(\mathbf{x}) a_j(\mathbf{x}) \tag{2}$$

where $p_j(\mathbf{x})$ is the jth basis (generally a monome), m ($m < N$) is the number of the bases, and $a_j(\mathbf{x})$ are the coefficients of each base. The m basis terms form the following m-dimensional vector:

$$P^{\mathrm{T}}(\mathbf{x}) = \{p_j(\mathbf{x})\}_{j=1}^{m}, \quad m < N \tag{3}$$

The vector $\mathbf{a}(\mathbf{x}) = [a_1(\mathbf{x}), \ldots, a_m(\mathbf{x})]^{\mathrm{T}}$ of the coefficients is obtained by solving a regression problem using the weighted least squares error $J(a(\mathbf{x}))$ for the N sampling points, defined as follows:

$$J(a(\mathbf{x})) = \sum_{i=1}^{N} w(\mathbf{x} - \mathbf{x}_i) \left[\sum_{j=0}^{m} p_j(\mathbf{x}_i) a_j(\mathbf{x}) - y_i \right]^2 \tag{4}$$

The minimization of the error $J(\mathbf{x})$ with respect to the coefficients $a_j(\mathbf{x})$ gives:

$$\mathbf{a}(\mathbf{x}) = \mathbf{A}^{-1}(\mathbf{x})\mathbf{B}(\mathbf{x})\mathbf{y} \tag{5}$$

where the matrix $\mathbf{A}$ and $\mathbf{B}$ are defined by:

$$\mathbf{A}(\mathbf{x}) = \sum_{i=1}^{N} w(\mathbf{x} - \mathbf{x}_i)\mathbf{p}(\mathbf{x}_i)\mathbf{p}^{\mathrm{T}}(\mathbf{x}_i) \tag{6}$$

$$\mathbf{B}(\mathbf{x}) = [w(\mathbf{x} - \mathbf{x}_1)\mathbf{p}(\mathbf{x}_1), \ldots, w(\mathbf{x} - \mathbf{x}_n)\mathbf{p}(\mathbf{x}_n)] \tag{7}$$

To guarantee the non-singularity of $\mathbf{A}$, for a point $\mathbf{x}$, an adequate support $B(\mathbf{x}_i)$ for each sample point $\mathbf{x}_i$ is needed so that $w(\mathbf{x} - \mathbf{x}_i) \neq 0$ for at least m experimental points [17].

The expression of the global approximation is

$$\tilde{y}(\mathbf{x}) = \mathbf{P}^{\mathrm{T}}(\mathbf{x})\mathbf{A}^{-1}(\mathbf{x})\mathbf{B}(\mathbf{x})\mathbf{y} \tag{8}$$

2.3. Adapting the experimental domain for the MLS approximation

The experimental domain D is a discrete one and is defined by the three-dimensional points $\mathbf{x}(J, p, T) \in D$. It includes experimental points at two operating fuel cell temperature values (50 °C and 70 °C) and at three values of the air pressure (1, 3 and 5 atm) achieved in the experimental conditions mentioned in Section 2.1. It is apparent that the experimental domain is included in the approximation domain $D \subset \tilde{D}$.

To adapt the experimental data with the MLS approximation, a support domain $B(\mathbf{x}_i)$ is considered around each experimental point. Thus, an entity is introduced to associate each experimental point $\mathbf{x}_i$ with a scalar r value, by which the support domain can be defined. This support can be constructed either by using a sphere

$$S_I = \{\mathbf{x} || \mathbf{x} - \mathbf{x}_I| < r\} \tag{9}$$

or, a n-dimensional cube:

$$S_I = \{\mathbf{x} || \mathbf{x}_i - \mathbf{x}_{I,i}| < r,\ 1 \leq i \leq n\}. \tag{10}$$

To ensure the computational feasibility and the accuracy of the application the following issues are requested:

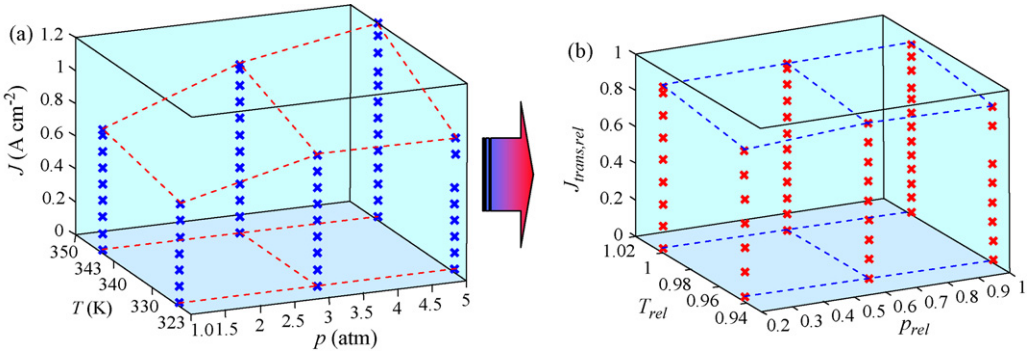

Fig. 2. Adapting experimental domain: (a) initial domain; (b) transformed domain.

1. each point of the approximation domain $\tilde{D}$ must be included in m compact supports, built around the experimental points, where m represents the number of bases;
2. a correct sizing of the compact supports, because an outsized support S_I of the function $w(\mathbf{x}-\mathbf{x}_i)$ would corrupt the local character of the approximation;
3. the experimental points included in the compact supports must be as uniformly distributed as possible according to each coordinate.

Taking into account the previously mentioned criteria the initial experimental domain has been transformed, obtaining a new domain (Fig. 2a and b), where the experimental points are more uniformly distributed. First of all, the parameters temperature and pressure have been normalized ($T_{\max} = 343$ K, $p_{\max} = 5$ atm) obtaining the relative values T_{rel} and p_{rel}. Since the relative temperature T_{rel} and the relative pressure p_{rel} are uniformly distributed, only the current density J has been first transformed and then normalized. The transformation is a linear one with moving coefficients which depend on the parameters T_{rel} and p_{rel}. This transformation is given by the following relationship:

$$J_{\text{trans}} = \frac{1}{a_1 \cdot T_{\text{rel}} + a_2} \cdot \frac{J}{\tanh(p_{\text{rel}} + b_1 \cdot T_{\text{rel}} + b_2)} \tag{11}$$

$$J_{\text{trans,rel}} = \frac{J_{\text{trans}}}{\max(J_{\text{trans}})} \tag{12}$$

In Eq. (11) the values of the coefficients are:

$$\begin{cases} a_1 = 7.7175 \\ a_2 = -6.3675 \\ b_1 = -3.9445 \\ b_2 = 4.3645 \end{cases}$$

The expression of the transformation function has been chosen to have almost a uniform transformed domain. To achieve this goal the examination of the experimental domain D has been made at first. Then a hyperbolic function has been chosen as the base of the transformation function. The coefficients of the transformation function have been computed accordingly to obtain a transformed domain, which is almost a rectangular polyhedron. Fig. 3 illustrates the steps, which have been followed at this stage.

The approximation method has been applied in the new transformed domain and then the inverse operation has been made to return to the initial domain.

3. Results

After pre-processing the experimental data, the MLS method can be applied to approximate the stationary characteristic of the PEMFC.

To estimate the accuracy of the method, the average of the global error for all the experimental points is given. The expression of this error is, in percentage:

$$\bar{\varepsilon}_{\text{g}} = \frac{100}{N} \sum_{i=1}^{N} \left| \frac{\tilde{V}(\mathbf{x}_i) - V(\mathbf{x}_i)}{V(\mathbf{x}_i)} \right| \tag{13}$$

where $\mathbf{x}_i = (J_i, p_i, T_i) \in D$, and N is the number of the experimental points. The computed value is $\bar{\varepsilon}_{\text{g}} = 1.62\%$. In Figs. 4–7 the symbols '×' represent the experimental dataset (the cell potential vs. current density with T, p as parameters) and the solid line represents the MLS approximation of the experimental data. Figs. 4 and 5 show the approximated fuel cell characteristics in the experimental conditions (Section 2.1). The two figures illustrate that the developed model fits with accuracy the experimental dataset.

However, the true interest of the method is the prediction and the description of the fuel cell behaviour in all of the points of the approximation domain. To prove these facilities the procedure of "cross-validation" [20] is used.

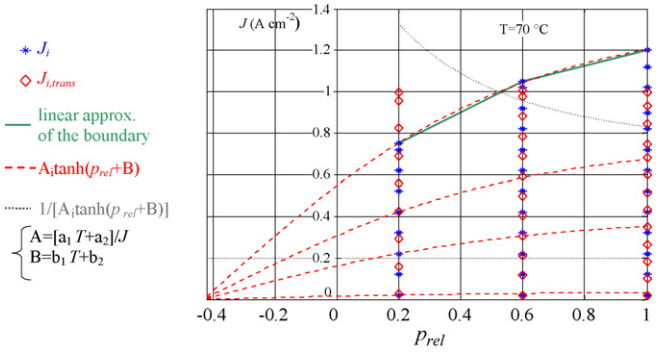

Fig. 3. Explanatory for the choosing process of the transformation function.

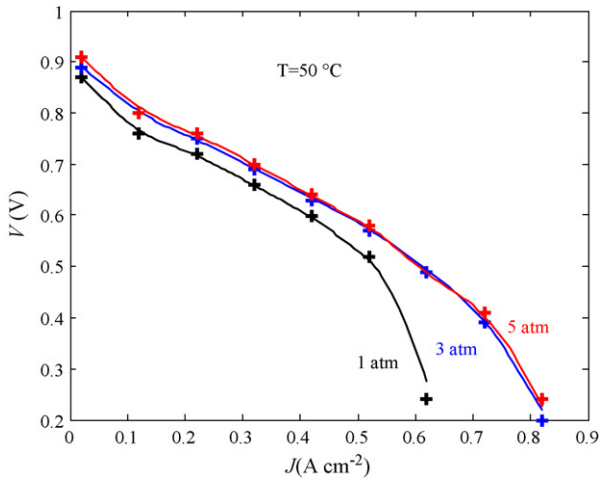

Fig. 4. Fuel cell voltage approximated characteristic, at $T = 50\,^{\circ}C$, for three different pressures: 1, 3 and 5 atm ('+' experimental data).

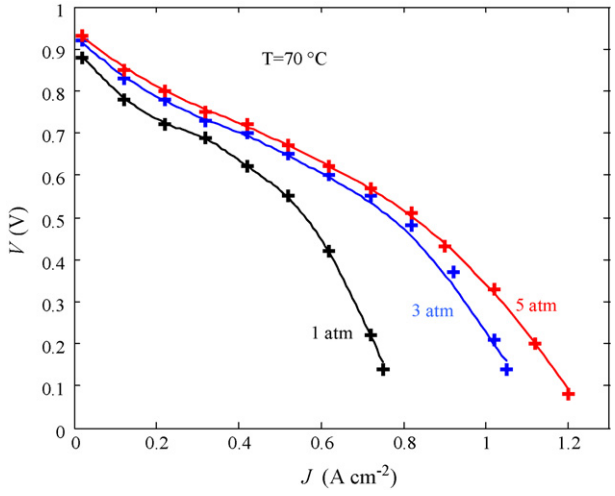

Fig. 5. Fuel cell voltage approximated characteristic, at $T = 70\,^{\circ}C$, for three different pressures: 1, 3 and 5 atm ('+' experimental data).

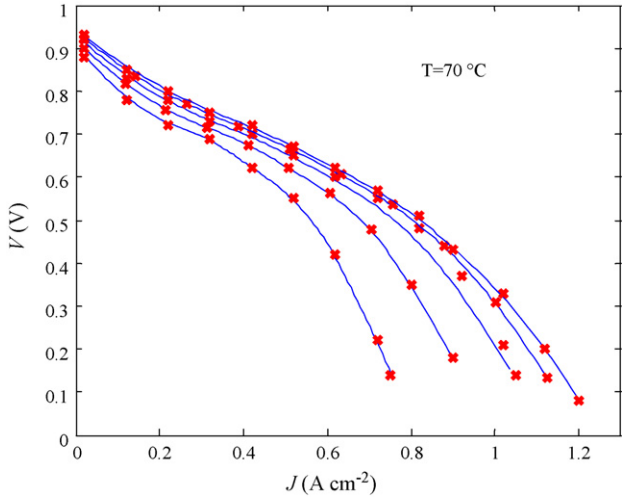

Fig. 6. Fuel cell voltage approximated characteristic with predicted data for 2 and 4 atm.

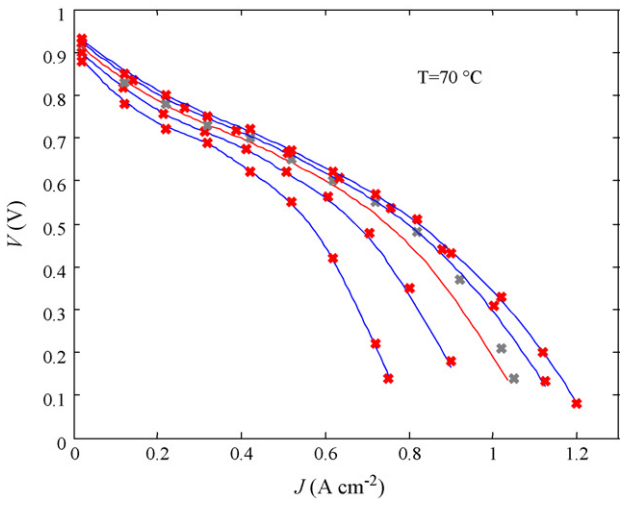

Fig. 7. Fuel cell voltage approximated characteristic with the 3 atm data points exclusion.

The experimental dataset is split into D_S distinct segments [20]. Then the approximation is made using data from $D_S - 1$ of the segments and its performance is tested using the remaining segments. Thus, another experiment is made by excluding experimental points. Starting from this reduced experimental domain the characteristic curve is reconstructed. This reconstruction includes the curve corresponding to the excluded points.

Fig. 6 shows the approximated results for five operating air pressures 1, 2, 3, 4, 5 atm at 70 °C fuel cell temperature. For "cross-validation" 40 new points (20 for 50 °C temperature and the others 20 for 70 °C temperature), which have been obtained from the approximated results for 2 and 4 atm, have been added at the initial dataset. Then the experimental real points for the 3 atm pressure have been excluded. Fig. 7 shows the approximated results obtained by the exclusion of the experimental real points for the 3 atm pressure and proves the accuracy of the prediction of the fuel cell performance in the whole approximation domain.

Fig. 8 shows, as a comparison, the error waveforms in case all the experimental data set were taken into account and in case all the dataset, without the input points of the 3 atm curve, were considered. The both curves have the same rate that proves the

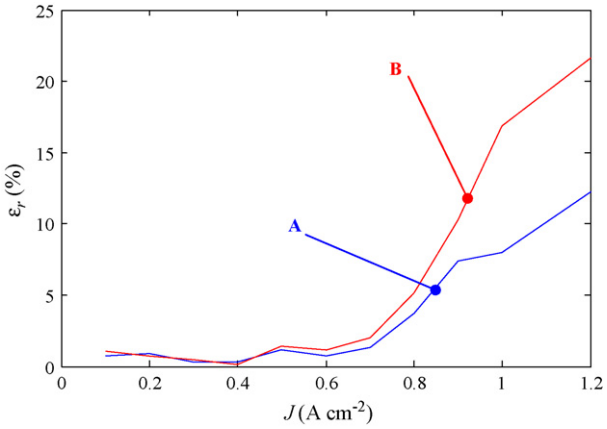

Fig. 8. The comparative analysis of the errors for the two cases: (A) all the dataset; (B) the dataset without the input points for 3 atm pressure.

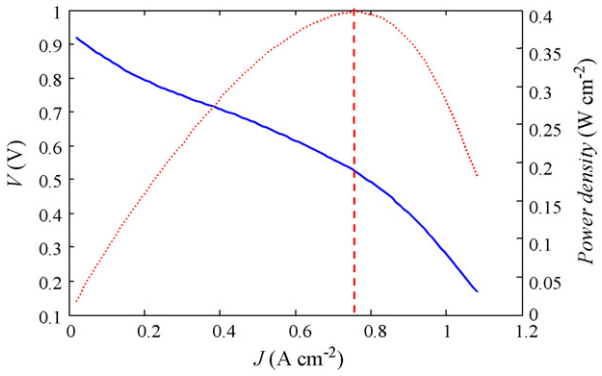

Fig. 9. Fuel cell voltage predicted characteristic and the cell power density (dotted line), at $T = 70\,^{\circ}C$ and $p = 3$ atm.

coherence of the proposed method. Of course, the first is lower, but they both grow with the current density in the non-linear region. The dispersion of the experimental points and the great values of the gradient on the domain boundary proximity are the reasons of this fact. The error can decrease if additional experimental points are introduced. Anyway, this part of the domain is not interesting for the fuel cell operation. As is shown in Fig. 9 the power density attains the maximum value before this region and the fuel cell operate at acceptable efficiencies before this point.

4. Conclusions

This paper proposes and develops a numerical method for modelling fuel cells with the help of moving least squares. The use of MLS is justified by the fact that it is a powerful method for approximating experimental data. The proposed model belongs to the family of surrogate models.

In conclusion, it can be said that:

- the proposed methodology is suitable for modelling PEMFC starting from experimental data. It also can be easily used to approximate the fuel cell behaviour for more input parameters than the temperature and pressure (stoichiometry, membrane humidity);
- the initial experimental domain must be transformed to obtain a new domain, where the distances between experimental points are more uniformly along the coordinates, to ensure both the convergence and the accuracy of the method;
- the validation of the method has been made using the procedure of "cross-validation". It is based on the graphical results and relative errors estimation. The level of the relative errors shows the goodness of this approach;
- the method can be improved to obtain a better precision in the neighbourhood of the domain boundary by adjusting the compact supports associated to the experimental points;
- the PEMFC static characteristics can be predicted and used for the development of the global model of the fuel cell system.

References

[1] U.S. Department of Energy Office of Fossil Energy, National Energy Technology Laboratory Morgantown, West Virginia, Fuel Cell Handbook (Sixth Edition), DOE/NETL-2002/1179 By EG&G Technical Services Inc. Science Applications International Corporation, November 2002.
[2] Cogeneration & On-Site Power Production, 8, Issue 1 January/February 2007, News.
[3] K. Haraldsson, K. Wipke, J. Power Sources 126 (2004) 88–97.
[4] D. Cheddie, N. Munroe, J. Power Sources 147 (2005) 72–84.
[5] T.E. Springer, T.A. Zawodzinski, S. Gottesfeld, J. Electrochem. Soc. 138 (8) (1991) 2334–2342.
[6] J. Kim, S. Lee, S. Srinivasan, Ch.E. Chamberlin, J. Electrochem. Soc. 142 (No. 8) (1995) 2670–2674.
[7] J.C. Amphlett, R.M. Baumert, R.F. Mann, B.A. Peppley, P.R. Roberge, J. Electrochem. Soc. 142 (No. 1) (1995) 1–8.
[8] R.F. Mann, J.C. Amphlett, M.A.I. Hooper, Heidi M. Jensen, B.A. Peppley, P.R. Roberge, J. Power Sources 86 (2000) 173–180.
[9] Ou Shaoduan, L.E.K. Achenie, J. Power Sources 140 (2005) 319–330.
[10] S. Busquet, C.E. Hubert, J. Labbé, D. Mayer, R. Metkemeijer, J. Power Sources 134 (2004) 41–48.
[11] B.D. Youn, K.K. Choi, Comput. Struct. 82 (2004) 241–256.
[12] N.V. Queipo, R.T. Haftka, W. Shyy, T. Goel, R. Vaidyanathan, P.K. Tucker, Progr. Aerospace Sci. 41 (2005) 1–28.
[13] T. Krishnamurthy, V.J. S Romero, 43rd AIAA/ASME/ASCE/AHS/ASC Structures, Structural Dynamics and Materials Conference, Denver, Colorado AIAA-2002-1466, 22–5 April, 2002, pp. 1–11.
[14] J.W. Bandler, Q.S. Cheng, A.S. Dakroury, A.S. Mohamed, M.H. Bakr, K. Madsen, J. Søndergaard, IEEE Trans. Microwave Theory Tech. 52 (2004) 337–360.
[15] P. Lancaster, K. Salkauskas, Mathematics of Computation, vol. 37, No. 155, Academic Press Inc., 1981, pp. 141–158.
[16] T. Belytschko, Y. Lu, L. Gu, Int. J. Numer. Methods Eng. 37 (1994) 229–256.
[17] C.A. Duarte, J.T. Oden. A Review of Some Meshless Methods to Solve Partial Differential Equations, Technical Report 95-06, TICAM, The University of Texas at Austin, May 1995.
[18] T. Ebner, C. Magele, B.R. Brandstatter, K.R. Richter, IEEE Trans. Magn. 34 (1998) 2928–2931.
[19] K. Rashid, E.M. Freeman, J.A. Ramirez, 3rd Brazilian Conf. Electromagn., Sao Paulo, Brazil, 1998.
[20] M. Stone, J. R. Stat. Soc. B 36 (1974) 111–147.